ORIGINAL RESEARCH

The influence of exocyclic lone pairs on the bonding and geometry of type A mesoionic rings

Christopher Antony Ramsden[1] · Wojciech Piotr Oziminski[2]

Abstract
Based on structures determined by X-ray crystallography, ab initio MP2 calculations on type A mesoionic rings give geometries in good agreement with observed values. A study of four mesoionic ring systems, each with exocyclic oxygen, nitrogen or carbon groups, shows that the presence and configuration of exocyclic lone pairs significantly influences the geometry and configurational preference. Using a localised bond model and NBO analysis, these effects are rationalised in terms of an anomeric interaction of lone pairs with the antibonding orbitals of adjacent σ bonds. In agreement with experiment, similar effects are calculated for pyran-2-imines.

Introduction

To investigate the influence of exocyclic lone pairs on the geometries, bonding and relative energies of type A mesoionic rings, we have studied four ring systems, each with exocyclic C=O, (E) and (Z) C=NPh and C=C(CN)$_2$ groups, using ab initio Moller-Plesset MP2 calculations. Early studies of the sydnones **1** did not support a polarised structure **1a** in which the ring is associated with an aromatic sextet. The C-O stretching frequencies (1768 cm^{-1}) and the exocyclic C-O bond lengths (1.20 and 1.215 Å) from X-ray studies are more consistent with the structure **1b** [1–3]. Another notable feature is the deformation of the bond angles C-C-O (135.7 and 135.5°) and O-C-O (119.2 and 121.2°). Thiessen and Hope in a study of 4,4'-dichloro-3,3'-ethylenebissydnone pointed out that the ring C-O bond (1.407 Å) is significantly longer than that in furan (1.362 Å) [2, 3]. This led these authors to suggest that the resonance structure **1c** contributes to the unusual bond lengths and bond angles. They also implied a participation of the carbonyl oxygen lone pairs leading to a contribution from structures **1d** resulting in shortening of one C-O bond and lengthening of the other [2].
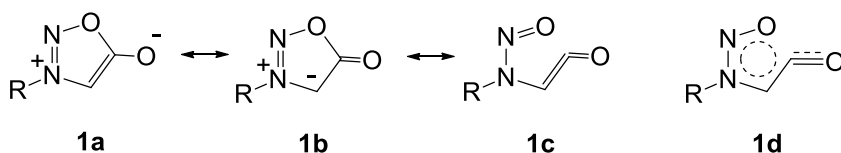
Type A mesoionic heterocycles are five-membered rings that can only be represented by dipolar structures and in which the ring heteroatoms formally contributing two electrons to the π-system have a 1,3 relationship; those with a 1,2 relationship are type B [4, 5]. The unusual bond lengths and angles in the sydnones **1** are recurring features of the geometries of type A mesoionic rings with an exocyclic oxygen. This is illustrated by comparing the crystal structures **2-5** (Fig. 1) [1, 6–8].

✉ Christopher Antony Ramsden
  c.a.ramsden@keele.ac.uk

✉ Wojciech Piotr Oziminski
  wojciech.oziminski@wum.edu.pl

1 Lennard-Jones Laboratories, School of Physical and Geographical Sciences, Keele University, Keele, Staffordshire ST5 5BG, UK

2 Faculty of Pharmacy, Medical University of Warsaw, 1 Banacha Street, ,02-097 Warsaw, Poland

2[1]   **3**[6]   **4**[7]   **5**[8]
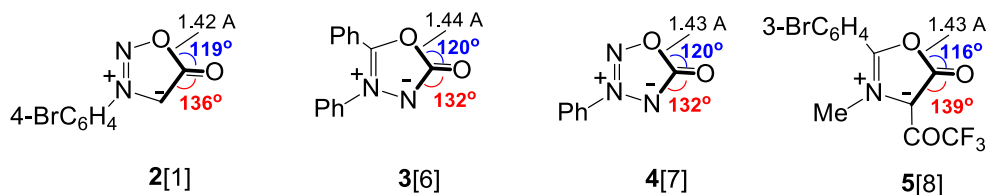
Similar bond angle distortions are seen in the crystal structure of the well-known analytical reagent nitron **6** (Fig. 2), which is a type A mesoionic ring with an exocyclic imine function [9]. During a casual examination of the crystal structure of the azasydnone imine **7** [10], we noticed two significant differences. In structure **7** the exocyclic angles are almost equal and, in contrast to nitron **6**, the imine **7** has the opposite configuration. Steric effects probably force nitron to adopt the observed configuration. Since there are no obvious steric interactions in imine **7**, we presumed this adopts the most stable configuration and that this preference may be attributable to the orientation of the exocyclic nitrogen lone pair. Three other crystal structures of mesoionic imines have been reported [11–13]. In two 1,3-diazol-4-imines, of which structure **8** is typical, steric effects also control the configuration. However, the 1,2,3-thiadiazol-5-imine **9** [13], in which steric effects are minimal (as in imine **7**), also has the opposite configuration to nitron **6**. We now report calculations that demonstrate the influence of the configuration of lone pairs on structural properties.

Results and discussion

Table 1 shows calculated bond lengths and angles for the mesoionic 1,2,3-oxadiazole and 1,2,3,4-oxatriazole derivatives **10a-d** and **11a-d**. The configurations of the imines are defined as *cis* or *trans* by the relationship of the nitrogen lone pair to the ring C-O or C-NR bond; the use of Cahn-Ingold-Prelog (CIP) *E* and *Z* nomenclature to define configuration varies with the ring system under consideration and is not a consistent terminology for comparing a series of hetero-rings.

Mesoionic rings with an exocyclic C=C(CN)$_2$ group are known [14–17]. We regard the enes **10d** and **11d** as structures that are not modified by the effects of exocyclic lone pairs and which, therefore, can be used as structural reference points. The effects of lone pairs are measured relative to these geometries. In Tables 1 and 2, φ_{15} and φ_{45} are the differences
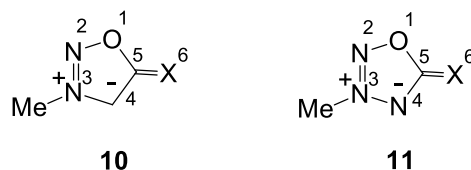
between the bond lengths in structures **10a-c** and **11a-c** and the corresponding bond lengths in **10d** and **11d**. Similarly, δ_{156} and δ_{456} measure the differences in the corresponding bond angles. The value Δ_{exo} is the difference between the exocyclic angles 1-5-6 and 4-5-6 for each structure. ΔG_{rel} are the relative free energies of the imine configurational isomers **10b,c** and **11b,c**.

The calculated gas phase geometries are in satisfactory agreement with the crystal structures **2**, **4** and **7** (Figs. 1 and 2). Inspection of Table 1 reveals that lone pairs increase the length of the 1-5 bond (φ_{15}) but the effect of a *trans* lone pair (**10c** and **11c**) is greater and the effect of two lone pairs (**10a** and **11a**) is greatest. A smaller and opposite effect is seen for the 4-5 bond (φ_{45}); here the larger effect is for the *cis* lone pair and the effects are not additive. The bond angles are also influenced by the configuration of the lone pair. *Trans* lone pairs increase angle 1-5-6 (δ_{156}) and decrease angle 4-5-6 (δ_{456}); *cis* lone pairs have the opposite effect. Inspection of the values of Δ_{exo} indicates that *trans*-imines have the smallest calculated difference between the exocyclic angles and *cis*-imines have the largest difference. This observation is consistent with the experimentally determined structure **6**. It is also significant to note that the *trans* isomers **10c** and **11c** are calculated to be the most stable (ΔG_{rel}) in accord with structure **7**.

In a parallel study, we have calculated the properties of the 1,3-diazoles **12** and the 1,3,4-triazoles **13**. Relevant structural properties are shown in Table 2. There is good agreement with the observed geometries of aryl analogues of **12a** [18], **12b** [11, 12] and **13b** [9]. Comparison with the data in Table 1 reveals similar trends, with notable differences that can be attributed to differences in C-O and C-NMe bonds. Changes in the ring bonds (φ_{15} and φ_{45}) show the same trends but the effects are smaller for φ_{15}. Trends in bond angle change with exocyclic group (δ_{156} and δ_{456}) are comparable in the two series as are the values of Δ_{exo}. However, it is notable that for the imines **12b,c** and **13b,c** the *cis* isomers are of lower energy (ΔG_{rel}). This is in agreement with the crystal structures of rings **6** and **8** (Fig. 2), and can be attributed to steric

6[9]   **7**[10]   **8** (Ar = 2,6-di^{i}PrC$_6$H$_3$)[12]   **9**[13]
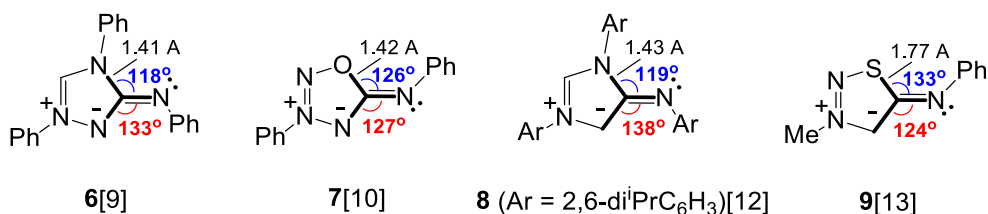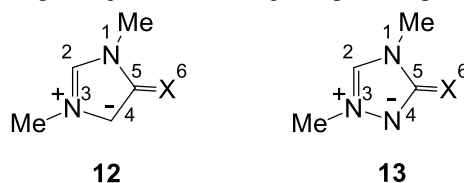
Table 1 MP2 calculated properties of the mesoionic rings **10** and **11**. [a]kcal mol^{-1}; [b]φ = difference in bond length compared to the corresponding bond length in structure **d**; [c]δ = difference in bond angle compared to the corresponding bond angle in structure **d**


10   **11**

Entry		Bond Lengths (Å)					Bond Angles (°)					
10	X	5-6	1-5	ϕ_{15}[b]	4-5	ϕ_{45}[b]	1-5-6	δ_{156}[c]	4-5-6	δ_{456}[c]	Δ_{exo}	ΔG_{rel}[a]
a	O	1.216	1.475	0.086	1.427	0.015	121.2	-0.6	137.4	+4.7	+16.2	-
b	cis-NPh	1.295	1.424	0.035	1.428	0.016	118.3	-3.5	138.0	+5.3	+19.7	0.0
c	trans-NPh	1.293	1.455	0.066	1.419	0.007	127.3	+5.5	130.1	-2.6	+2.8	-0.71
d	C(CN)$_2$	1.392	1.389	-	1.412	-	121.8	-	132.7	-	+10.9	-
11	X	5-6	1-5	ϕ_{15}[b]	4-5	ϕ_{45}[b]	1-5-6	δ_{156}[c]	4-5-6	δ_{456}[c]	Δ_{exo}	ΔG_{rel}[a]
a	O	1.206	1.471	0.077	1.390	0.016	122.0	-0.2	133.0	+4.2	+11.0	-
b	cis-NPh	1.273	1.440	0.046	1.396	0.022	117.5	-4.7	136.4	+7.6	+18.9	0.0
c	trans-NPh	1.279	1.455	0.061	1.388	0.014	127.8	+5.6	126.3	-2.5	-1.5	-0.72
d	C(CN)$_2$	1.380	1.394	-	1.374	-	122.2	-	128.8	-	+6.6	-

interactions in the *trans* isomers. In the *trans* isomers **12c** and **13c** the NPh rings are twisted away from planarity (30-40°) indicating energetically unfavourable interactions. Although the *cis* isomer **13b** is fully planar, the Ph group is also twisted in the *trans* isomer **13c** indicating steric interaction with C^{4}H that is absent when replace by N^4.

Using the localised bonding model, we rationalise the observed properties in terms of energetically favourable anomeric effects between the exocyclic lone pairs and the antibonding orbitals of the adjacent ring bonds. In the *trans* configuration **14** the lone pair overlaps with the antibonding orbital of the C-Ẍ bond (n→σ_{CX}*) (Fig.

Table 2 MP2 calculated properties of the mesoionic rings **12** and **13**. [a]kcal mol^{-1}; [b]φ = difference in bond length compared to the corresponding bond length in structure **d**; [c]δ = difference in bond angle compared to the corresponding bond angle in structure **d**

12   **13**

Entry		Bond Lengths (Å)					Bond Angles (°)					
12	X	5-6	1-5	ϕ_{15}[b]	4-5	ϕ_{45}[b]	1-5-6	δ_{156}[c]	4-5-6	δ_{456}[c]	Δ_{exo}	ΔG_{rel}[a]
a	O	1.248	1.445	0.048	1.432	0.016	123.2	-3.9	134.6	+6.5	+11.4	-
b	cis-NPh	1.325	1.416	0.019	1.434	0.018	117.7	-9.4	138.9	+10.8	+21.2	0.0
c	trans-NPh	1.328	1.432	0.035	1.422	0.006	126.5	-0.6	130.0	+1.9	+3.5	+3.9
d	C(CN)$_2$	1.423	1.397	-	1.416	-	127.1	-	128.1	-	+1.0	-
13	X	5-6	1-5	ϕ_{15}[b]	4-5	ϕ_{45}[b]	1-5-6	δ_{156}[c]	4-5-6	δ_{456}[c]	Δ_{exo}	ΔG_{rel}[a]
a	O	1.237	1.442	0.041	1.387	0.017	123.5	-3.4	130.4	+5.8	+6.9	-
b	cis-NPh	1.312	1.421	0.020	1.389	0.019	117.7	-9.2	135.4	+10.8	+17.7	0.0
c	trans-NPh	1.313	1.433	0.032	1.382	0.012	127.3	+0.4	125.7	+1.1	-1.6	+5.2
d	C(CN)$_2$	1.411	1.401	-	1.370	-	126.9	-	124.6	-	+2.3	-
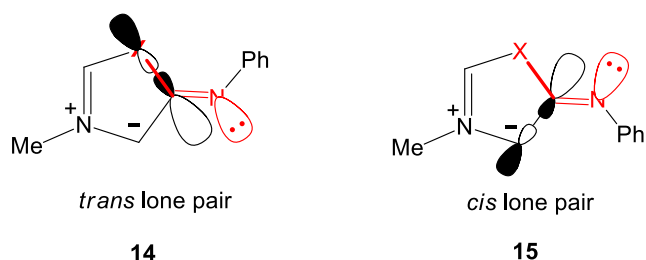
Fig. 3 Anomeric interactions between *trans* and *cis* lone pairs on adjacent ring bonds

3). This stabilising interaction introduces an antibonding element into the C-$\ddot{X}$ bond resulting in bond lengthening (φ_{15} positive) while reinforcing the exocyclic C=N bond. The overlap shown in structure **14** is probably increased by increasing the angle 1-5-6 (δ_{156} positive). In accord with general bond properties, the size of the antibonding lobe on the C^5 carbon will be related to the polarity of the bond and will increase as the electronegativity of $\ddot{X}$ increases. This is consistent with the observation of a greater effect in the C=NPh *trans* structures **10c** and **11c** (C-O bond) than in **12c** and **13c** (C-NMe bond) (Tables 1 and 2).

A similar analysis (Fig. 3, Structure **15**) accounts for the effect of a *cis* lone pair on bond lengths and angles. In this case the *cis* lone pair interacts with the antibonding orbital of the C-C or N-C ring 4-5 bond. Again, the greatest effects are on the more polar N-C bonds (**11b** and **13b**). In the cases where the exocyclic atom is oxygen, both lone pairs influence the geometry. For the 1-5 bonds there is an additive effect but for the 4-5 bonds the combined effect is not significant. For the angles 1-5-6 and 4-5-6 there is a compromise between the effects of *cis* and *trans* lone pairs and Δ_{exo} has an intermediate value.

The anomeric effects described here are analogous to other hyperconjugative effects between the antibonding orbitals of polar bonds and adjacent lone pairs, which often account for conformational preferences [5]. Anomeric effects are sometimes attributed to dipolar or steric interactions. In the case of type **A** mesoionic structures these effects seem unlikely; the derivatives **11**, which have similar dipolar and steric characteristics regardless of configuration, have a similar profile to the other derivatives **10**, **12** and **13**. Within the localized bond model, other orbital interactions obviously influence relative energy and geometry. However, we believe that those shown in Fig. 3 dominate. It is also important to recognise that, in addition to lone pairs, other factors influence ring geometries. These include the nature of ring heteroatoms as can be seen from the variation of Δ_{exo} for the dicyano derivatives (**10d** – **12d**, Tables 1 and 2).
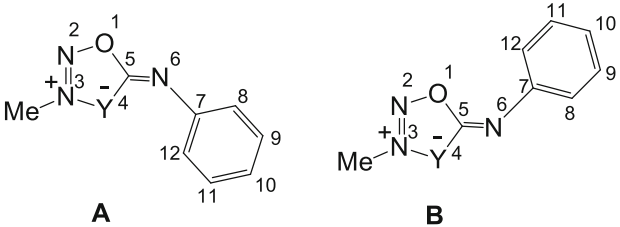
To support the model summarised in Fig. 3, we have carried out a Natural Bond Order (NBO) analysis for the configurational isomers **10b,c** and **11b,c**. The results for the most significant nitrogen lone pair interactions are shown in Table 3, where the relationships of structures **A** and **B** to **10b,c** and **11b,c** are shown. Inspection of Table 3 reveals that by far the strongest interactions are between the N6 lone pair and the C5-O1 σ* orbital in structures **B** (Entries 1 and 5). These interactions are much larger (33.24 and 34.53 kcal mol^{-1}) than the other lone pair interactions in **A** or **B**. This stabilisation energy is sufficient to account for the preferred configurations in structures **7** and **9**, in which steric effects are minimal, and are in good agreement with the localised bond model shown in Fig. 3.

It is significant to note that in **11b** (**A**; Y = N) the stabilisation for lone pair interaction with the N4-C5 σ* orbital (21.66 kcal mol^{-1}) (Entry 6) is greater than for interaction with the less polar C4-C5 σ* orbital in **10b** (**A**; Y = CH) (15.17 kcal mol^{-1}) (Entry 2). However, this is not sufficient to outweight the large interactions with C5-O1 σ*. The stronger lone pair interaction with the σ* orbitals of polar C-O and C-N bonds (Table 3) are also consistent with the calculated variations in bond length (Tables 1 and 2) and the observed bond lengths in Type A mesoionic rings.

We regard the dicyano derivatives as a realistic choice of reference structure. Analogues of this type are known [14–17, 19, 20], and the exocyclic group C=C(CN)$_2$ is a good lone pair-free electronic analogue of C=O and C=NAr. Unsubstituted derivatives C=CH$_2$ are of some interest for two reasons: (i) mesoionic examples of this type were prepared and fully characterised (with X-ray structures) in 2020 [21]; (ii) the CH bonds may show some hyperconjugative electron donation, in a manner analogous to lone pairs.

Table 4 compares calculated properties of C=C(CN)$_2$, *cis* and *trans* C=CHCN and C=CH$_2$ mesoionic 1,3-diazoles **16**. The results reveal some evidence of C-H hyperconjugation, especially by the *trans* CH bond in structure **16c**. Although the effects of the CH bonds in structures **16** are less than those of lone pairs, the trends in bond length and bond angle change are similar, and this suggests an analogous but smaller anomeric effect. The isomer **16c** is less stable (ΔG_{rel}) than **16b**, and this is attributable to a small steric interaction between Me and CN.

The structure of the CH$_2$ derivative **16a** is of particular interest since, unlike the other mesoionic rings which are planar, the five-membered ring in structure **16a** shows distortion from planarity in both the calculated and X-ray structures (torsion angle 1-5-4-3: calc. 4.4°; obsd 4.2°). This can be attributed to an increased π electron population introducing anti-aromatic character. The index pEDA (pi Electron Donor-Acceptor) is the sum of

Table 3 Significant NBO stabilisation energies E^2 and orbital energy. Differences $E(j)$-$E(i)$ for the Configurational Isomers **A** and **B**. [a]kcal mol^{-1}; [b]a.u.
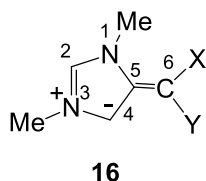

Entry	Donor(i)	Acceptor(j)	$E^{(2)a}$	$E(j)$-$E(i)^b$	$E^{(2)a}$	$E(j)$-$E(i)^b$
			10b (**A**; Y = CH)		**10c** (**B**; Y = CH)	
1	N6 lone pair	O1-C5 σ*	7.23	0.60	33.24	0.53
2	N6 lone pair	C4-C5 σ*	15.17	0.83	2.13	0.82
3	N6 lone pair	C7-C12 σ*	4.98	0.90	9.74	0.88
4	N6 lone pair	C7-C8 σ*	0.0	0.0	0.0	0.0
			11b (**A**; Y = N)		**11c** (**B**; Y = N)	
5	N6 lone pair	O1-C5 σ*	10.51	0.54	34.53	0.52
6	N6 lone pair	N4-C5 σ*	21.66	0.71	4.57	0.73
7	N6 lone pair	C7-C12 σ*	9.38	0.89	9.62	0.88
8	N6 lone pair	C7-C8 σ*	1.23	0.90	1.37	0.89

the populations of the ring p_z atomic orbitals minus the aromatic sextet value of six [22]. The pEDA values for the ene structures **16a-d** are shown in Table 3. The π-electron ring population of **16a** is demonstrably higher than the cyano derivatives **16b-d** and also the oxygen and nitrogen derivatives **12a-c** (pEDA: **12a** 0.230; **12b** 0.262; **12c** 0.192). Overall the dicyano derivatives have comparable properties to oxygen and nitrogen analogues and are realistic hyperconjugation-free references structures for studying the influence of lone pairs.

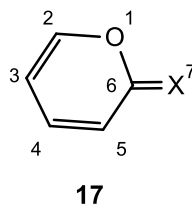To explore whether similar anomeric effects are found in other heterocyclic rings with exocyclic substituents, we have calculated properties of the pyrone derivatives **17a-d**. *N*,4,6-Triphenypyran-2-imines are known [23, 24], and Uncuţa and coworkers, in a detailed NMR study, have shown that in equilibrium mixtures, e.g., **17b,c**, the *trans* (*Z*) configuration prevails [25].

Examination of Table 5 reveals that the structural changes in the series **17a-d** are similar to the trends in Tables 1 and 2. It is noteworthy that the angle difference Δ_{exo} is smallest for the *trans* isomer **17c** (+1.8°) and largest for the *cis* isomer **17b** (+15.0°); this closely parallels the analogous structures **10** and **11** (Table 1). In agreement with experimental data [25], the *trans* isomer **17c** is calculated to be the more stable (ΔG_{rel} -0.23 kcal mol^{-1}) (Table 5).

Table 4 MP2 calculated properties of the mesoionic rings **16**. [a]kcal mol^{-1}; [b]φ = difference in bond length compared to the corresponding bond length in structure **d**; [c]δ = difference in bond angle compared to the corresponding bond angle in structure **d**

16

Entry			Bond Lengths (Å)					Bond Angles (°)						
16	X	Y	5-6	1-5	ϕ_{15}^b	4-5	ϕ_{45}^b	1-5-6	δ_{156}^c	4-5-6	δ_{456}^c	Δ_{exo}	ΔG_{rel}^a	pEDA
a	H	H	1.384	1.417	0.020	1.442	0.026	124.4	-2.7	132.7	+4.6	+8.3	-	0.402
b	H	CN	1.402	1.403	0.006	1.426	0.010	124.2	-2.9	131.7	+3.6	+7.5	0.0	0.281
c	CN	H	1.405	1.408	0.011	1.427	0.011	126.4	-0.7	129.9	+1.8	+3.5	+1.2	0.267
d	CN	CN	1.423	1.397	-	1.416	-	127.1	-	128.1	-	+1.0	-	0.166

Table 5 MP2 calculated properties of the pyrone derivatives **17a-d.** [a]kcal mol^{-1}; [b]φ = difference in bond length compared to the corresponding bond length in structure **d**; [c]δ = difference in bond angle compared to the corresponding bond angle in structure **d**

17

Entry		Bond Lengths (Å)					Bond Angles (°)					
17	X	6-7	1-6	ϕ_{16}[b]	5-6	ϕ_{56}[b]	1-6-7	δ_{167}[c]	5-6-7	δ_{567}[c]	Δ_{exo}	ΔG_{rel}[a]
a	O	1.218	1.420	0.046	1.458	0.018	117.4	+1.5	127.4	+2.2	+10.0	-
b	cis-NPh	1.294	1.398	0.024	1.457	0.017	114.0	-1.9	129.0	+3.8	+15.0	0.0
c	trans-NPh	1.295	1.404	0.030	1.451	0.011	120.6	+4.7	122.4	-2.8	+1.8	-0.23
d	C(CN)$_2$	1.387	1.374	-	1.440	-	115.9	-	125.2	-	+9.3	-

Conclusions

MP2 calculated geometries of type A mesoionic rings are in good agreement with reported crystal structures. *Cis* and *trans* lone pairs on the exocyclic heteroatoms have different effects on bond lengths, bond angles and total energies. For exocyclic imino groups (C=NAr), in the absence of steric effects, the *trans* configuration is favoured energetically. Within the localised bond model, these effects are rationalised in terms of anomeric interactions of lone pairs with the antibonding orbitals of adjacent σ bonds, resulting in bond lengthening. These results provide some insight into the structures of type A mesoionic rings which generally have a short exocyclic bond and a particularly long ring C-Ẍ heterobond (e.g., **1b**), rather than a ring associated with an aromatic sextet (e.g., **1a**). In agreement with experiment, similar structural effects are seen in pyrone derivatives.

Computational details

Calculations were performed using the Gaussian 16 program [26] at the ab initio Moller-Plesset MP2 level of theory [27]. The correlation consistent aug-cc-pVDZ (ACCD) basis set was used [28, 29]. All geometry optimizations were followed by frequency calculations to establish the nature of the stationary point and to calculate the ZPE and thermal corrections to Gibbs free energy. All minima on the Potential Energy Surface have no imaginary frequencies. For the analysis of possible orbital donor→acceptor interactions the Natural Bond Orbital (NBO) analysis was performed [30]. The stabilization energies accompanying the most important delocalizations were estimated via second-order perturbative method.

The NBO method applied was 3.1 implemented in Gaussian 16. Because the MP2 density matrix cannot be analysed for delocalizations, the B3LYP/aug-cc-pVDZ density matrix (based on MP2/aug-cc-pVDZ optimized structures) was employed.

Declarations

References

1. Bärnighausen H, Jellinek F, Munnik J, Vos A (1963). Acta Cryst 16:471
2. Thiessen WE, Hope H (1967). J Am Chem.Soc 89:5977
3. Hope H, Thiessen WE (1969). Acta Cryst B25:1237
4. Ollis WD, Ramsden CA (1976). Adv Heterocycl Chem 19:1
5. Katritzky AR, Ramsden CA, Joule JA, Zhdankin VV. Handbook of Heterocyclic Chemistry Third Edn. Elsevier Oxford 2010 p. 35-36
6. King TJ, Preston PN, Suffolk JS, Turnbull K (1979). J Chem Soc Perkin Trans 2:1751
7. Ottersen T (1975). Acta Chem Scand A29:799
8. Boyd GV, Davies CG, Donaldson JD, Silver J, Wright PH (1975). J Chem Soc Perkin Trans 2:1280
9. Cannon JR, Raston CL, White AH (1980). Aust J Chem 33:2237
10. Ottersen T, Christophersen C, Treppendahl S (1975). Acta Chem Scand A29:45
11. César V, Tourneux J-C, Vujkovic N, Brousses R, Lugan N, Lavigne G (2012). Chem Commun 48:2349
12. Danopoulos AA, Monakhov KY, Braunstein P (2013). Chem Eur J 19:450
13. Kozinskij VA, Zelenskaja OV, Bruckner S, Malpezzi L (1984). J Heterocycl Chem 21:1889
14. Grashey R, Baumann M (1969). Angew Chem Int Ed 8:133
15. Grashey R, Baumann M, Hamprecht R (1970). Tetrahedron Lett 11:5083
16. Grashey R, Baumann M (1972). Tetrahedron Lett 13:2947
17. Hanley RN, Ollis WD, Ramsden CA, Smith IS (1979). J Chem Soc Perkin Trans 1:744
18. Biju A, Hirano K, Fröhlich R, Glorius F (2009). Chem Asian J 4: 1786
19. Newton CG, Ollis WD, Wright DE (1984). J Chem Soc Perkin Trans 1:69
20. Jaźwiński J, Kamieński B, Staszewska-Krajewska O, Webb GA (2003). J Mol Struct 646:1
21. Hansmann MM, Antoni PW, Pesch H (2020). Angew Chem Int Ed 59:5782
22. Ozimiński WP, Dobrowolski JC (2009). J Phys Org Chem 22:769
23. Van Allen JA, Chie Chang S (1974). J Heterocycl Chem 11:1065
24. Afridi AS, Katritzky AR, Ramsden CA (1977). J Chem Soc Perkin Trans 1:1436
25. Uncuța C, Tudose A, Căproiu MT, Udrea S (2003). Arkivoc (i):29
26. Gaussian 16 Revision B.01 Frisch MJ, Trucks GW, Schlegel HB, Scuseria GE, Robb MA, Cheeseman JR, Scalmani G, Barone V, Petersson GA, Nakatsuji H, Li X, Caricato M, Marenich AV, Bloino J, Janesko BG, Gomperts R, Mennucci B, Hratchian HP, Ortiz JV, Izmaylov AF, Sonnenberg JL, Williams-Young D, Ding F, Lipparini F, Egidi F, Goings J, Peng B, Petrone A, Henderson T, Ranasinghe D, Zakrzewski VG, Gao J, Rega N, Zheng G, Liang W, Hada M, Ehara M, Toyota K, Fukuda R, Hasegawa J, Ishida M, Nakajima T, Honda Y, Kitao O, Nakai H, Vreven T, Throssell K, Montgomery Jr JA, Peralta JE, Ogliaro F, Bearpark M J, Heyd JJ, Brothers EN, Kudin KN, Staroverov VN, Keith TA, Kobayashi R, Normand J, Raghavachari K, Rendell AP, Burant JC, Iyengar SS, Tomasi J, Cossi M, Millam JM, Klene M, Adamo C, Cammi R, Ochterski JW, Martin RL, Morokuma K, Farkas O, Foresman JB, Fox DJ. Gaussian Inc. Wallingford CT 2016
27. Møller C, Plesset MS (1934). Phys Rev 46:618
28. Dunning Jr TH (1989). J Chem Phys 90:1007
29. Woon DE, Dunning Jr TH (1993). J Chem Phys 98:1358
30. Foster JP, Weinhold F (1980). J Am Chem Soc 102:7211